Time dilation effects in micron-size rotating optical Ferris-wheel traps

V. E. Lembessis,[1,*] J. Yuan,[2] K. Köksal,[3,4] and M. Babiker[2]

[1]*Photonics Group, Department of Physics and Astronomy, College of Science, King Saud University, Riyadh 11451, Saudi Arabia*

[2]*School of Physics Engineering and Technology, University of York, York YO10 5DD, United Kingdom*

[3]*Physics Department, Bitlis Eren University, Bitlis, Turkey*

[4]*Faculty of Engineering and Natural Sciences, Gaziantep Islam Science And Technology University, Gaziantep, Turkey*

(Received 3 March 2025; accepted 25 August 2025; published 6 October 2025)

Advances in lasers and atomic clock technologies have enabled delicate measurements to be made of minute relativistic effects. Here, we propose that such developments should lead to the measurement of relativistic effects involving atoms and molecules in dynamic optical traps. Specifically, we make a case for the study of time dilation in the context of atoms and molecules trapped in a rotating optical Ferris wheel. With experimentally relevant examples, we demonstrate how this would extend relativity tests down to the micron scale and would constitute a potential advance toward micron-size Mössbauer-style spectroscopy for trapped atoms and molecules.

DOI: 10.1103/5m6c-hfqt

I. INTRODUCTION

Recently, a number of experimental initiatives [1,2] have been launched aiming to reveal possible violations or breakdown of quantum principles or the relativity principles and, partly, in order to set experimental limits on the departures from the predictions of the existing theories. For example, a possible breakdown of the equivalence principle of general relativity has been tested using the free fall of the atomic wave packets in the presence of terrestrial Earth gravity [2]. Also, the effect of gravity on the decoherence of entangled photons has been investigated in a space-based experiment [1]. Furthermore, the IceCube collaboration has carried out measurements on the possible effect of Earth's gravity on the superposition of muons [3]. An important positive common feature of such research is that it has involved terrestrial laboratory-based experiments, which ensures their accessibility and repeatability. Such research also complements the above-mentioned aim of exploring the possible new physics at smaller scales.

The remarkable progress in the physics of cold atoms and molecules in recent decades has highlighted the system of trapped cold atoms as an ideal laboratory platform for investigating a number of physical effects [4]. Trapped atoms and ions have long been used in the realization of atomic clocks for the purpose of accurate timekeeping [5]. They provide ideal tools for the measurement of time dilation arising from special and general relativity effects. A notable achievement is the measurement of time dilation due to relative linear motion, which is as slow as a walking pace of 10 m/s, and the gravitational time dilation due to height differences of the order of tens of centimeters (33 cm) using trapped ions [6]. Trapped neutral atoms in an optical lattice have been used to set the current record for gravitational time dilation measurement arising from elevations of a few centimeters [7] and millimeters [8], achieving a sensitivity of 10^{-18} [9].

In this article, we propose to use trapped neutral atoms or molecules, henceforth both referred to as "atoms," in a rotating optical Ferris wheel as clocks to measure the time dilation arising when the atoms are trapped in a rotating potential well. The quantum states of the atoms can be engineered to be coherent over the micron dimensions of the optical Ferries wheel. This makes the proposed platform distinct from the platforms adopted in all previous experiments where the clocks are sufficiently localized to be treated as particle-like.

This article begins with a brief introduction of relativistic effects in a rotating frame and their implementation using a rotating optical Ferries-wheel system, and we show that it is possible to trap atoms and molecules with high, albeit nonrelativistic, angular speed using experimentally feasible setups. We then show different schemes in which time dilation effects can be measured to probe the dynamics of the trapped atoms, enabling tests of relativity physics. Finally, we highlight some of possible experimental challenges involved.

II. BACKGROUND

Relativistic effects in rotating frames are well known from the very beginning of the development of relativistic physics but still generate a lot of intense discussions [10] because they involve effects which can be interpreted both in terms of special relativity involving observers at rest relative to the rotating frame and in terms of a noninertial frame for an observer embedded in the rotating frame. For example, the time dilation of a clock localized at a radial distance ρ from the center of a rigid disk rotating with an angular frequency Ω, as measured

*Contact author: jun.yuan@york.ac.uk

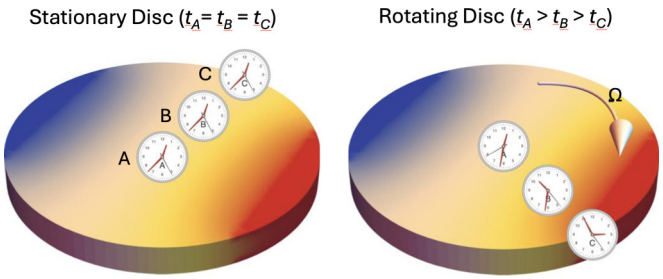

FIG. 1. Different time dilations experienced by clocks located at different positions on a disk rotating at a constant angular speed Ω, as viewed by an observer in the local (nonrotating) inertial frame of reference.

by an observer at rest [i.e., in an inertial (laboratory) frame], can be understood in terms of the tangential speed $v = \Omega\rho$ of the clock (see Fig. 1). This so-called kinematic time dilation is given by $\tau(\rho) = \gamma\tau_0$, with $\gamma = 1/\sqrt{1 - \Omega^2\rho^2/c^2}$ and τ_0 the proper time of a clock in the rotating frame while τ is the time measured by a stationary (inertial) observer. This has been verified by lifetime measurements of elementary particles in storage ring experiments, such as the muon experiments at CERN [11] and also at Brookhaven [12] with $v \sim c$.

An alternative experimental approach is to measure the corresponding frequency shift of the atomic resonance [13,14] or that of the nucleus [15,16], which is also the basis of successful satellite navigation systems such as the Global Positioning System (GPS) [17]. The fractional change in the measured frequency is given by

$$\frac{f - f_0}{f_0} = \frac{1}{\gamma} - 1, \sim \frac{v^2}{2c^2} = k\frac{\Omega^2\rho^2}{c^2}, \tag{1}$$

where k is a parameter, f is the resonance frequency of the rotating atom, and f_0 is that for an atom at rest in the laboratory frame. This result is valid in the nonrelativistic limit where $v \ll c$ with $k = 0.5$.

However, for an observer embedded with the rotating frame, there is no relative motion, and yet the Mössbauer rotor experiments, involving the self-absorption effect of two atomic clocks, clearly demonstrated the time dilation of the same magnitude for both clocks. As observers in any rotating frame would experience centrifugal and Coriolis forces, one can attribute the observed time delay as the result of centrifugal acceleration $a = -\Omega^2\rho = -v^2/\rho$, as the Coriolis force is velocity dependent and can be ignored here. We can then rewrite Eq. (1) as

$$\frac{f - f_0}{f_0} \sim k\frac{\Omega^2\rho^2}{c^2} = -k\frac{a\rho}{c^2}. \tag{2}$$

Einstein used this example to introduce the theory of general relativity for gravity through the Einstein equivalence principle (EEP), which states that the effects of gravity are locally indistinguishable from the effects of acceleration [18]. Indeed, artificial gravity due to the rotation of spaceships is a proposed engineering solution against the weightless environment of space stations. Above the Earth's surface, the Newtonian gravity force on a particle of mass m_g is given by $F_n = Gm_gM_E/(R + h)^2$, where M_E and R are the mass and the radius of the Earth and G is the gravitational constant. This means that the acceleration due to gravity at a height h above the surface is $GM_E/(R + h)^2 \sim g(1 - 2h/R)$, where $g = GM/R^2$. Thus, there is also time dilation for a clock at height h above the Earth's surface relative to a clock localized on the surface:

$$\frac{f(h) - f_0}{f_0} \sim = 2k'\frac{gh}{c^2}, \tag{3}$$

where $2k' = 1$ if the Earth's rotation is not taken into account [17]. For satellites such as those used in GPS, time dilation due to satellites orbiting the Earth and that due to different gravity acceleration at its orbit with respect to that on the ground are both important to arrive at the precise location.

Until now, quantitative tests of relativity involving rotating systems have been carried out at the centimeter scale and above. We now show that a similar relativity test platform can be generated using rotating optical Ferris wheels in the micron scale [19,20].

III. RELATIVISTIC EFFECTS IN A ROTATING FERRIS-WHEEL TRAP

A. Rotating optical Ferris wheels

An optical Ferris wheel is essentially an optical lattice with cylindrical symmetry. It can be created by the interference of two co-propagating Laguerre-Gaussian (LG) modes: $LG_{p,\ell}$ and $LG_{p,-\ell}$. Here, p and ℓ are the radial and azimuthal indices of the LG modes [21]. The nonzero value of ℓ is also called the winding number. The Ferris wheel refers to the resulting intensity pattern $I(\rho, \phi)$ at the focal plane where both LG modes have their minimum beam waist w_0:

$$I(\rho, \phi) = I_0\left(\frac{2\rho^2}{w_0^2}\right)^{\ell} \exp\left(-\frac{2\rho^2}{w_0^2}\right) L_{p,\ell}^2\left(\frac{2\rho^2}{w_0^2}\right) \times \cos^2\left(\ell\phi + \frac{\delta}{2}t\right), \tag{4}$$

where w_0 is the waist parameter and $L_{p,\ell}$ is the associated Laguerre polynomial. The overall factor I_0 is given by

$$I_0 = \frac{PC_{p,\ell}^2}{\pi w_0^2}, \tag{5}$$

where P is the overall power distributed among the two LG beams and $C_{p,\ell} = \sqrt{p!/(p + |\ell|)!}$ is a normalization factor, which is equal to 1 in the case of $\ell = 1$, $p = 0$.

The detuning of the angular frequency of one of the beams ($\omega_2 = \omega_1 + \delta$) results in a rotation of the transverse light intensity pattern at the rate $\Omega = \delta/2\ell$ [19]. Alternatively, the spatial light modulator (SLM) responsible for the LG beam generation can be made to rotate [20]. The sense of the rotation can be changed by changing the sign of angular frequency difference δ if two laser beams are employed.

B. Rotating Ferris-wheel trapping potential

Atoms and molecules with dc polarizability α_s are attracted to the most intense part of the light field at the focal plane by

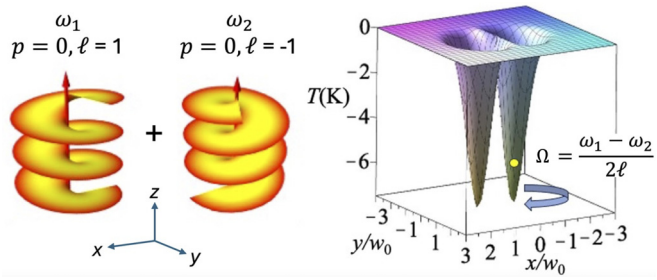

FIG. 2. A rotating optical Ferris-wheel trap can be realized in the minimum beam waist w_0 of the superposition of $LG_{p,\ell}$ and $LG_{p,-\ell}$ beams copropagating along the z direction, as shown here for $\ell = 1$ and $p = 0$. The transverse intensity pattern in the (x, y) plane has a two-loop structure within which atoms or molecules can be trapped, with trapping along the z direction ensured by tweezing mechanisms [20].

the dipole force. The relevant dipole potential is given by

$$U = -\frac{\alpha_s I}{2\epsilon_0 c} = -k_B T C^2_{p,|\ell|} \frac{I}{I_0}, \tag{6}$$

where ϵ_0 is the permittivity of free space and I the averaged intensity over a period of the light field. In Eq. (6), and in what follows, we have chosen to express the depth of the trapping potential in terms of the effective temperature, i.e., Kelvin degree T.

In Fig. 2 we present the dipole potential wells due to a rotating Ferris wheel made of two LG modes: $LG_{0,1}$ and $LG_{0,-1}$. There are two trapping regions which rotate like a two-dimensional dumbbell at an angular velocity equal to $\Omega = \delta/2$. The frequency shift δ between the two laser beams can be controllably set by the use of an acoustic modulator, with δ adjustable to values up to gigahertz.

C. Time-dilation effect

The time dilation of these atomic clocks can be probed by Doppler spectroscopy of a well-defined internal electronic transition [6]:

$$\frac{f'}{f_0} = \frac{1 - \beta\cos\theta}{\sqrt{1-\beta^2}} \simeq (1 - \beta\cos\theta)\left(1 + \frac{\beta^2}{2}\right), \tag{7}$$

where θ is the angle between the direction of the velocity of the source with respect to the line of sight between the atom and the observer, $\beta = \rho\Omega/c$, and f' is the measured frequency, which includes the first-order Doppler shift effect. If we choose to collect light emitted in the z direction ($\theta = 90^o$) by a stationary detector, then we can measure the second-order Doppler effect, i.e., the time dilation induced frequency change in Eq. (1) directly.

D. Deep QUEST potential

In a rotating optical Ferris wheel a trapped atom or molecule experiences a centrifugal force which can be sufficiently large to eject the atom or molecule out of its trap. It is therefore essential that the trapping potential is very deep.

Conventional optical dipole traps for atoms have trap depths limited to the mK range, due to the trade-off between trapping and radiative scattering, both of which are functions of the detuning of the dipole resonance [22]. The quasi-electrostatic optical trap (QUEST) proposed by Singh *et al.* [23] may provide traps as deep as 10 K. QUEST achieved this by using the dc polarizability of the atoms and molecules in their ground state (i.e., effectively large detuning with negligible scattering and very high laser intensity that can be realized in an optical cavity [24]). The use of a cold buffer gas facilitates the cooling and loading of the trapped species, overcoming the limit of laser cooling. In the following, we evaluate the QUEST trap characteristics using nitrogen gas molecules as a realistic example. Although the trapping characteristics are not state dependent as is the case of resonant dipole trapping, the principles we have followed in the case of nitrogen also apply to other molecules and atoms with a sizable dc polarizability and a large ionization potential [23].

IV. CASE STUDIES

A. Rotating $p = 0$, $\ell = 1$ Ferris-wheel QUEST trap

For simplicity we consider the simplest Ferris wheel for which $\ell = 1$ and $p = 0$. Figure 2 shows a QUEST trapping potential for nitrogen molecules, generated with two suitably detuned LG beams of wavelength $\lambda = 1064$ nm and a common beam waist $w_0 = 4 \times 10^{-6}$ m, i.e., $w_0 = 3.8\lambda$. We assume that the power is chosen such that the trapping potential depth is 7.5 K. This consists of two trapping regions that can be made to rotate about the center of the beam at $\rho = 0$. At the radial position where a stationary trapping potential is minimum, namely, $\rho_0 = w_0\sqrt{\ell/2}$, we can adopt the harmonic potential approximation (see Appendix A):

$$U(\rho, \phi, z) \sim \frac{M}{2}\omega_\rho^2(\rho - \rho_0)^2\cos^2(\ell\phi) - \frac{M}{2}\Omega^2\rho^2, \tag{8}$$

where M is the mass of the atom or the molecule in the trap, ω_ρ is the angular frequency characterizing the spring constant of the harmonic potential, and the second term in the potential is due to the fictitious centrifugal force on the trapped atoms or molecules, now seen from the perspective of the rotating Ferris wheel. Trapping in the z direction is also assumed and not included here. When the centrifugal potential (at ρ_0) equals the depth of the trapping potential (at rest), the atoms or molecules will escape from the trap. The maximum angular velocity that could keep the molecule trapped in this case is $\Omega_{\max} = 1.3 \times 10^7$ rad/s.

To avoid escaping, we may consider a smaller angular speed $\Omega = 2 \times 10^6$ rad/s, which is achieved when the frequency shift between the beams is $|\delta| = 2\pi \times 6.4 \times 10^5$ rad/s. In this case we have $\frac{\Delta f}{f_0} = 4 \times 10^{-16}$, if the trapped atom stays at $\rho = \rho_0$. However, the presence of rotation will modify the radial harmonic frequency to $\sqrt{\omega_\rho^2 - \Omega^2}$ and modifies the equilibrium radial position by the factor $\omega_\rho^2/(\omega_\rho^2 - \Omega^2)$ while reducing the depth of the harmonic trapping potential by the residual centrifugal potential contribution at the trap minimum (see Appendices). This slight change in the equilibrium radial position will contribute to a modification

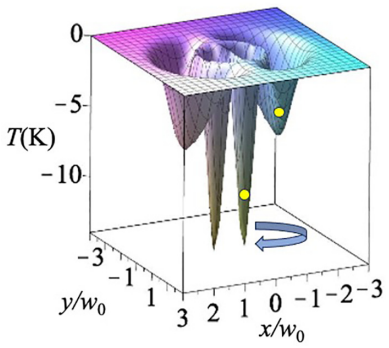

FIG. 3. Trapping potential (in Kelvin degrees) created by a rotating Ferris wheel with $\ell = 1$ and $p = 1$.

of the frequency shift given in Eq. (1):

$$\frac{f(\Omega) - f_0}{f_0} \sim \frac{\Omega^2}{2c^2}\rho_{\text{eff}}^2 \sim \left(1 + \frac{2\Omega^2}{\omega_\rho^2}\right)\frac{\Omega^2}{2c^2}\rho_0^2. \tag{9}$$

In our example, the rotational angular velocity is much smaller than the radial harmonic frequency of the deep trap. We obtain $(\Omega/\omega_\rho)^2 \approx 0.003$. So the fractional frequency shift due to elasticity of the trap is only 0.6%.

At the micron scale, the motion of the center of mass should be treated quantum mechanically, with associated position uncertainty. Assuming that the trapped particles are cooled sufficiently to be confined to the ground state of the radial quantum harmonic oscillator, we can estimate the radial position uncertainty from the ground-state wave function: $\langle\Delta\rho\rangle = \sqrt{\hbar/2M\omega_\rho}$. The ground-state energy for this trapped molecule, when there is no rotation, is 220 μK and the uncertainty in its position is $\langle\Delta\rho\rangle \approx 5.5 \times 10^{-9}$ m, which contributes a tiny spectral broadening of the relative frequency change of 0.4 %. This ground-state energy is also much larger than the recoil energy (of the order of μK), effectively ensuring recoil-free transitions.

B. Rotating $p = 1$, $\ell = 1$ Ferris-wheel QUEST trap

Another use of the Ferris-wheel platform is to test the dependence of the kinematic time dilation on the radial position of the trapped atoms or molecules. This makes use of a rotating trapping potential profile, which is created by the superposition of two LG modes of $\ell = \pm 1$, $p = 1$ as shown in Fig. 3. We have two concentric Ferris wheels of different radii ($\rho = 0.47w_0$ and $1.5w_0$, respectively). The same angular speed will cause different radial accelerations for the trapped atoms in the traps. The rotational rate to use is determined by considerations of the shallower external trapping well, and $\Omega = 2 \times 10^6$ rad/s is sufficient to ensure deep trapping at this site since the maximum allowed rotation is $\Omega_{\text{max}} = 1.4 \times 10^7$ rad/s. The internal trapping site has a deeper potential, so this will not be a concern. For the QUEST beam parameters stated above, the trap characteristics can be estimated and are listed in Table I of Appendix B. The main difference is that the frequency values of the signals emitted by trapped molecules can be measured in a single experimental run, therefore minimizing the temporal fluctuation of the experimental setup in the experimental verification of Eq. (1). In fact, if a superposition of LG beams can be used, such as in a perfect vortex beam [25], the radial positions of the trapping potential can be decoupled from the number of traps at the same radius (controlled by ℓ), giving an additional degree of flexibility.

C. Mössbauer-like experiments

With such deep particle traps, recoil-free Mössbauer-like experiments can be carried out involving internal electronic excitations of the trapped atoms or molecules, by studying resonance energy transfer between two atoms or molecules embedded at different radii of the rotating system. This is a direct analog of the case involving energy transfer between two recoil-free nuclei in classical Mössbauer experiments (Refs. [15] and [16], for example). This may be achieved by setting up a rotating Ferris-wheel light using a far-off-resonance laser, together with a weak coaxial near-resonance Gaussian light trap. The particles in the on-axis trap act as sources of resonance fluorescence transfer to the off-center rotating particles. As the speed of light in such a noninertial system is not constant [10], Corda suggests that the effective value of k in Eq. (2) is then equal to $2/3 \sim 0.67$ [26] on account of the resulting clock synchronization effect alone, while other explanations have been proposed [27]. Traditionally, the measured frequency shift in a Mössbauer experiment is directly interpreted using $k = 0.5$ in Eq. (2), despite the fact that the equation is specifically for a stationary observer. The independent experimental approach we have detailed here will contribute to the resolution of this issue and verify the recent reinterpretation of Kündig's Mössbauer results [28] and the related experimental work [27]. Mössbauer-like spectroscopy may also provide a possible means of measuring chemical shifts in the emerging field of "nanochemistry" using trapped atoms and molecules [23].

D. Gravity effects

Finally, we can compare the time dilation due to radial acceleration with that due to gravity on the Earth's surface. As a guide to orders of magnitude: two identical clocks on the surface of the Earth separated by a vertical distance z have a relative frequency shift gradient $\Delta f/f_0 = -1.019 \times 10^{-16}$ m^{-1} [8]. This is of the order of magnitude of the ratios that can be achieved with angular speeds of the order of 10^6 rad/s. It means that we can ignore the gravitational tidal effect over the Rayleigh length of the LG beams ($\pi w_0^2/\lambda$), which is of the order of a micron meter. We can ensure that the plane of the Ferris wheel is always horizontal to minimize possible gravity gradient effects in the kinematic time dilation experiment. On the other hand, lifting the Ferris-wheel setup would then allow a repeat of the time dilation experiments at different elevations. This provides a check of the (local) equivalence principle by comparing the time dilation due to "artificial" gravity at the micron level due to the rotating Ferris wheel with those of curved space-time due to terrestrial gravity. We note that the radial acceleration involved in our case is of the order of $10^6 g$, comparable to the gravity found on the surfaces of white dwarfs and less massive neutron stars [29], and significantly larger than $100g$ achieved for a linear moving lattice [9] and an order of magnitude larger than that

achieved in a typical Mössbauer experiment [16]. Therefore, our approach offers a sensitive laboratory-scale artificial gravity platform when searching for a possible deviation from the standard physical understanding [30].

V. DISCUSSION

The broad applicability of the QUEST trapping is very helpful, as it allows a large number of atoms and molecular species to be considered for their suitability for high-precision clock experiments. Ideally, there needs to be a metastable transition with a long lifetime (τ), and it should be insensitive to environmental perturbation, specifically in our case the high laser intensity involved. For example, among many suitable candidates, the Xe neutral atom has a deeper QUEST potential due to its larger dc polarizability than that of N_2 and with a comparable ionization potential [23]. It has a suitable clock transition $6s[3/2]_2 - 6s'[1/2]_0$ [31] with an intrinsic decay rate of $7s^{-1}$ [32]. Often the achievable clock precision can be further improved by special engineering approaches [33] to reduce, for example, the differential Stark effect and the blackbody radiation from the optical components nearby, in the context of the high-laser-field environment. This is a subject of continuing research [34] and is specific to the atomic and molecular species under consideration, but it is outside the scope of this paper.

Furthermore, it is worth noting that the recent rapid development of tunable UV lasers may allow the use of metastable nuclear transitions to improve the ability to measure even smaller relative frequency changes [35]. By using these so-called optical nuclear clocks in the rotating Ferris-wheel setup, one can make a system of nuclear-clock-capable atoms or molecules trapped in a slower rotating Ferris-wheel platform also accessible for detailed study. The slower rotation of the Ferris wheel will also relax the need for a high-intensity-trapping laser and so reduce the issues associated with high intensity.

All the experiments proposed in this paper should constitute highly sensitive experimental platforms for resolving many existing controversies surrounding relativity in a rotating system [36] and for experimentally probing for possible deviations from the existing theoretical predictions due to the convergence of relativity and quantum mechanics [4], particularly at the level of the micron scale. For example, we have assumed that the "clock hypothesis," which states that the clock behaves the same whether it is in an inertial reference frame or in a noninertial frame, is valid. However, there are suggestions [37] that the energy-level spacing inside the atoms or molecules may be a function of the angular speed, thus rendering the clock postulate invalid. The rotating Ferris-wheel system proposed here can be an ideal test bed for the clock hypothesis and the ramifications in case it is not valid.

VI. CONCLUSIONS

In summary, we have shown that time dilation should now be measurable for atoms and molecules trapped in deep but realistic potential wells rotating with an angular velocity Ω as high as 10^6 rad/s. We have also derived a nonrelativistic correction to the frequency shift due to the centrifugal force and the elasticity of the trapping potential. The analysis provides a micron-scale test of relativistic effects and can, in principle, be combined with the manipulation of the quantum state of the trapped particles. Our approach leads to the direct measurement of the instantaneous rotational speed, which is important for the study of the phenomena of atom dynamics with nonuniform rotational speeds that may be controlled by the programed detuning of the laser beams. This contrasts with the average rotational speed of the atoms using the Sagnac effect [38] and the rotational speed of the Ferris wheel determined by laser frequency detuning.

ACKNOWLEDGMENTS

The authors are grateful to A. Singh for helpful correspondence concerning the dipole trapping of molecules in QUEST. We are also grateful to Aidan Arnold for the clarification of issues related to the experimental generation of optical Ferris wheels, and to B. Dash for the clarification of the dynamics of trapped particles in rotating traps.

DATA AVAILABILITY

The data that support the findings of this article are not publicly available. The data are available from the authors upon reasonable request.

APPENDIX A: EFFECTIVE HARMONIC MOTION IN A ROTATING FRAME

A particle radially trapped in a harmonic potential well experiences an additional centrifugal energy when the system is subject to rotation of angular frequents Ω. In cylindrical coordinates the total potential is

$$U(\rho,\phi) = \frac{M}{2}\omega_\rho^2(\rho-\rho_0)^2 - \frac{M}{2}\Omega^2\rho^2, \tag{A1}$$

where ρ_0 is the static equilibrium position. As a result of the rotation we have a new equilibrium position, ρ_0^{eff}, at the minimum point of the total potential. We have

$$\frac{dU}{d\rho} = 0 = M\omega_\rho^2\left(\rho_0^{\text{eff}} - \rho_0\right) - M\Omega^2\rho_0^{\text{eff}}. \tag{A2}$$

Rearranging leads to the expression for ρ_0^{eff}

$$\rho_0^{\text{eff}} = \frac{\omega_\rho^2}{\omega_\rho^2 - \Omega^2}\rho_0. \tag{A3}$$

If Ω^2/ω_ρ^2 is much smaller than unity, then we have $\rho_0^{\text{eff}} \approx (1 + \Omega^2/\omega_\rho^2)\rho_0$. Expanding out the square in Eq. (A1), we have

$$U(\rho,\phi) = \frac{M}{2}\omega_\rho^2\left(\rho^2 - 2\rho\rho_0 + \rho_0^2\right) - \frac{M}{2}\Omega^2\rho^2 \tag{A4}$$

or

$$U(\rho,\phi) = \frac{M}{2}\left[\left(\omega_\rho^2 - \Omega^2\right)\rho^2 - 2\rho\omega_\rho^2\rho_0 + \omega_\rho^2\rho_0^2\right)\Big]. \tag{A5}$$

This can be rewritten in the following form:

$$\frac{M}{2}\left(\omega_\rho^2 - \Omega^2\right)^2\left(\rho - \rho_\rho^{\text{eff}}\right)^2 - \frac{M}{2}\Omega^2\left(\rho_0^{\text{eff}}\right)^2, \tag{A6}$$

TABLE I. Rotating Farris-wheel trap parameters.

Traps	$\ell = 1, p = 0$	$\ell = 1, p = 1$ (outer trap)	$\ell = 1, p = 1$ (inner trap)
Escape angular rotational speed ($\Omega_{\max}$, rad/s)	1.3×10^7	1.4×10^7	2×10^6
Angular rotational speed (Ω, rad/s)	2×10^6	2×10^6	2×10^6
Uncorrected fractional frequency shift due to time dilation [$\frac{\Delta f}{f_0}$, Eq.(1)]	3.5×10^{-16}	8×10^{-16}	7.8×10^{-17}
Percentage Centrifugal correction factor to the pure-time dilation [Δ, Eq.(9)]	0.6%	0.043%	0.54%
Centrifugal correction to the pure-time dilation $\Delta(\frac{\Delta f}{f_0})$	2.1×10^{-19}	3.6×10^{-19}	4.2×10^{-19}
Radial harmonic frequency (ω_ρ, from fitting to the numerical simulation, rad/s)	3.65×10^7	6.4×10^8	4.7×10^7
Radial position uncertainty [σ_ρ, Eq. (A8), m]	5.5×10^{-9}	1.3×10^{-9}	5.0×10^{-9}
Radial position at rest (ρ_0), from the beam waist parameter	4×10^{-6}	6×10^{-6}	1.6×10^{-6}
Ground-state energy ($>0.5\hbar\omega_\rho$) from fitting to the numerical simulation (μK)	220	3400	260

which shows that the harmonic frequency is also modified to

$$\omega_\rho^{\text{eff}} = \sqrt{\omega_\rho^2 - \Omega^2} \tag{A7}$$

and the depth of the harmonic potential well is reduced by the centrifuge potential at the new equilibrium position.

For a particle confined to the ground state, the position uncertainty in the radial direction is given by

$$\sigma_\rho^2 = \langle(\Delta\rho)^2\rangle = \frac{\hbar}{2M\omega_\rho^{\text{eff}}}. \tag{A8}$$

If $(\Omega/\omega_\rho)^2 \approx 0.003$ and $\Omega = 2 \times 10^6$ rad/s, then $\omega_\rho \approx 3.65 \times 10^7$ rad/s. This gives $\sigma_\rho \approx 5.5 \times 10^{-9}$ m. With $\rho_0 = 3.8\lambda \approx 4 \times 10^{-6}$ m, we have $\sigma_\rho/\rho_0 \approx 0.0014$, hence the line broadening is given by $\sigma_f/f_0 = (\sigma_\rho/\rho)^2 \approx 1.9 \times 10^{-6}$. The time dilation frequency shift should then be measurable despite the the existence of this line broadening due to radial position uncertainty.

Also for Rb, the natural line width is 38 MHz, compared with the resonance frequency of 3.85×10^{14}, hence the ratio is 1/10 000, so the line broadening due to radial position uncertainty is more difficult to measure. But such a measurement may be utilized to infer the maximum occupation number of the particle in the harmonic trap.

APPENDIX B: TRAP PARAMETERS AND CHARACTERISTICS

The detailed parameters of the traps as shown in Figs. 2 and 3 are listed in Table I, together with the derived properties. The expected fractional time dilation is larger than the fractional gravitational time dilation that has been measured using atomic clocks [8,9]) i.e., $>10^{-18}$, and the recoil energy for N_2 molecules emitting at 780 nm (for order of magnitude estimate) [$>0.5\hbar\omega_\rho$, Eq. (8)] 0.7 μK. The simulation was done for a $\text{LG}_{\ell,p}$ beam with a minimum beam width of $w_0 = 4 \times 10^{-6}$m and of wavelength $\lambda = 1064$ nm.

[1] P. Xu, Y. Ma, J.-G. Ren, H.-L. Yong, T. C. Ralph, S.-K. Liao, J. Yin, W.-Y. Liu, W.-Q. Cai, X. Han, H.-N. Wu, W.-Y. Wang, F.-Z. Li, M. Yang, F.-L. Lin, L. Li, N.-L. Liu, Y.-A. Chen, C.-Y. Lu, Y. Chen *et al.*, Satellite testing of a gravitationally induced quantum decoherence model, Science **366**, 132 (2019).

[2] M. He, X. Chen, J. Fang, Q. Chen, H. Sun, Y. Wang, J. Zhong, L. Zhou, C. He, J. Li, D. Zhang, G. Ge, W. Wang, Y. Zhou, X. Li, X. Zhang, L. Qin, Z. Chen, R. Xu, Y. Wang *et al.*, The space cold atom interferometer for testing the equivalence principle in the China space station, npj Microgravity **9**, 58 (2023).

[3] The-ICECUBE-collaboration, Neutrino interferometry for high-precision tests of Lorentz symmetry with IceCube, Nat. Phys. **14**, 961 (2018).

[4] M. S. Safronova, D. Budker, D. DeMille, D. F. J. Kimball, A. Derevianko, and C. W. Clark, Search for new physics with atoms and molecules, Rev. Mod. Phys. **90**, 025008 (2018).

[5] D. McCarthy and K. Seidelmann, *Time: From Earth Rotation to Atomic Physics* (Wiley, New York, 2009).

[6] C.-W. Chou, D. B. Hume, T. Rosenband, and D. J. Wineland, Optical clocks and relativity, Science **329**, 1630 (2010).

[7] M. Takamoto, I. Ushijima, N. Ohmae, T. Yahagi, K. Kokado, H. Shinkai, and H. Katori, Test of general relativity by a pair of transportable optical lattice clocks, Nat. Photon. **14**, 411 (2020).

[8] T. Bothwell, C. J. Kennedy, A. Aeppli, D. Kedar, J. M. Robinson, E. Oelker, A. Staron, and J. Ye, Resolving the gravitational redshift across a millimetre-scale atomic sample, Nature (London) **602**, 420 (2022).

[9] X. Zheng, J. Dolde, V. Lochab, B. N. Merriman, H. Li, and S. Kolkowitz, Differential clock comparisons with a

multiplexed optical lattice clock, Nature (London) **602**, 425 (2022).
[10] O. Grøn, Relativistic description of a rotating disk, Am. J. Phys. **43**, 869 (1975).
[11] B. Rossi and D. B. Hall, Variation of the rate of decay of mesotrons with momentum, Phys. Rev. **59**, 223 (1941).
[12] F. J. M. Farley and E. Picasso, The muon (g-2) experiments, Annu. Rev. Nucl. Part. Sci. **29**, 243 (1979).
[13] J. C. Hafele and R. E. Keating, Around-the-world atomic clocks: Predicted relativistic time gains, Science **177**, 166 (1972).
[14] D. Hasselkamp, E. Mondry, and A. Scharmann, Direct observation of the transversal Doppler-shift, Z. Phys. A **289**, 151 (1979).
[15] H. J. Hay, J. P. Schiffer, T. E. Cranshaw, and P. A. Egelstaff, Measurement of the red shift in an accelerated system using the Mössbauer effect in Fe^{57}, Phys. Rev. Lett. **4**, 165 (1960).
[16] W. Kündig, Measurement of the transverse Doppler effect in an accelerated system, Phys. Rev. **129**, 2371 (1963).
[17] N. Ashby, Relativity in the global positioning system, Living Rev. Relativ. **6**, 1 (2003).
[18] A. Einstein, Über das relativitätsprinzip und die aus demselben gezogenen folgerungen, Jahrb. Radioakt. Elektron. **4**, 411 (1907).
[19] S. Franke-Arnold, J. Leach, M. J. Padgett, V. E. Lembessis, D. Ellinas, A. J. Wright, J. M. Girkin, P. Öhberg, and A. S. Arnold, Optical Ferris wheel for ultracold atoms, Opt. Express **15**, 8619 (2007).
[20] X. He, P. Xu, J. Wang, and M. Zhan, Rotating single atoms in a ring lattice generated by a spatial light modulator, Opt. Express **17**, 21014 (2009).
[21] L. Allen, M. W. Beijersbergen, R. J. C. Spreeuw, and J. P. Woerdman, Orbital angular momentum of light and the transformation of Laguerre-Gaussian laser modes, Phys. Rev. A **45**, 8185 (1992).
[22] C. Cohen-Tannoudji and D. Guéry-Odelin, *Advances in Atomic Physics: An Overview* (World Scientific, Singapore, 2011).
[23] A. Singh, L. Maisenbacher, Z. Lin, J. J. Axelrod, C. D. Panda, and H. Müller, Dynamics of a buffer-gas-loaded, deep optical trap for molecules, Phys. Rev. Res. **5**, 033008 (2023).
[24] C. Turnbaugh, J. J. Axelrod, S. L. Campbell, J. Y. Dioquino, P. N. Petrov, J. Remis, O. Schwartz, Z. Yu, Y. Cheng, R. M. Glaeser *et al.*, High-power near-concentric Fabry–Perot cavity for phase contrast electron microscopy, Rev. Sci. Instrum. **92**, 053005 (2021).
[25] P. Vaity and L. Rusch, Perfect vortex beam: Fourier transformation of a Bessel beam, Opt. Lett. **40**, 597 (2015).
[26] C. Corda, Interpretation of Mössbauer experiment in a rotating system: A new proof for general relativity, Ann. Phys. **355**, 360 (2015).
[27] A. Kholmetskii, T. Yarman, O. Yarman, and M. Arik, Comment on "Underlining possible effects of Coriolis acceleration in experiments with a Mössbauer source" by Benedetto Elmo et al., Europhys. Lett. **134**, 19002 (2021).
[28] A. L. Kholmetskii, T. Yarman, and O. V. Missevitch, Kündig's experiment on the transverse Doppler shift re-analyzed, Phys. Scr. **77**, 035302 (2008).
[29] B. W. Carroll and D. A. Ostlie, *An Introduction to Modern Astrophysics* (Cambridge University, Cambridge, 2017).
[30] W. Klink and S. Wickramasekara, Quantum mechanics in noninertial reference frames: Violations of the nonrelativistic equivalence principle, Ann. Phys. **340**, 94 (2014).
[31] U. Sterr, A. Bard, C. J. Sansonetti, S. L. Rolston, and J. D. Gillaspy, Determination of the xenon $6s[3/2]_2 - 6s'[1/2]_0$ clock frequency by interferometric wavelength measurements, Opt. Lett. **20**, 1421 (1995).
[32] M. Walhout, U. Sterr, A. Witte, and S. L. Rolston, Lifetime of the metastable $6s'[1/2]_0$ clock state in xenon, Opt. Lett. **20**, 1192 (1995).
[33] Y. Takahashi, C. Zhang, A. Jadbabaie, and N. R. Hutzler, Engineering field-insensitive molecular clock transitions for symmetry violation searches, Phys. Rev. Lett. **131**, 183003 (2023).
[34] D. DeMille, N. R. Hutzler, A. M. Rey, and T. Zelevinsky, Quantum sensing and metrology for fundamental physics with molecules, Nat. Phys. **20**, 741 (2024).
[35] K. Beeks, T. Sikorsky, T. Schumm, J. Thielking, M. V. Okhapkin, and E. Peik, The thorium-229 low-energy isomer and the nuclear clock, Nat. Rev. Phys. **3**, 238 (2021).
[36] *Relativity in Rotating Frames*, edited by G. Rizzi and M. L. Ruggiero (Springer, Netherlands, 2004).
[37] I. Bialynicki-Birula and Z. Bialynicka-Birula, Rotational frequency shift, Phys. Rev. Lett. **78**, 2539 (1997).
[38] B. Dash, M. H. Goerz, A. Duspayev, S. C. Carrasco, V. S. Malinovsky, and G. Raithel, Rotation sensing using tractor atom interferometry, AVS Quantum Science **6**, 014407 (2024).